J Biomol NMR (2014) 60:29–36
DOI 10.1007/s10858-014-9846-y

ARTICLE

Pairwise binding competition experiments for sorting hub-protein/effector interaction hierarchy and simultaneous equilibria

Enrico Ravera · Azzurra Carlon · Giacomo Parigi

Received: 23 April 2014 / Accepted: 5 July 2014 / Published online: 12 July 2014

Abstract NMR experiments on proteins in simultaneous equilibria with multiple binding partners can provide a tool to understand complex biological interaction networks. Competition among proteins for binding to signaling hubs is often at the basis of the information transmission across signaling networks in every organism. Changes in affinity towards one or more partners, as well as changes of the relative concentration of the competing partners, can determine pathways alterations that lead to pathological consequences. Overall, the knowledge of the interaction hierarchy of the multiple partners to a single signaling hub can lead to new therapeutic strategies. Smith and Ikura (Nat Chem Biol 10:223–230, 2014) have recently proposed pairwise competition NMR experiments to determine the binding hierarchy in network interactions. We have taken the moves from their approach to show how from pairwise competition NMR experiments the ratios between the equilibrium constants for multiple binding partners can be determined, and thus, given their concentration in solution, the concentrations of all the possible complexes can be obtained.

Keywords Simultaneous equilibria · Dissociation constants · RAS · Competition experiments · NMR

Electronic supplementary material The online version of this article (doi:10.1007/s10858-014-9846-y) contains supplementary material, which is available to authorized users.

E. Ravera · A. Carlon · G. Parigi (✉)
Magnetic Resonance Center (CERM) and Department of Chemistry "Ugo Schiff", University of Florence, Via L. Sacconi 6, 50019 Sesto Fiorentino, Italy
e-mail: parigi@cerm.unifi.it

Introduction

Unravelling the interaction networks among proteins is the ultimate goal of systems biology, with particular reference to the understanding of signaling pathways (Kholodenko et al. 2010; Kitano 2002; Papin et al. 2005). Signaling pathways involve sensing external stimuli (e.g. nutrients, hormones, growth factors) at receptor level and transmitting the biological information within the cell through regulation of its activities. This information is encoded by changes in concentration, structure and localization of proteins and other molecules, and is processed by a complex cascade of biochemical reactions. Due to this complexity, the detailed investigation of signaling pathways requires direct and quantitative experimental access to many of the molecules involved in the interaction network. In particular, proteins involved in a competitive binding with multiple partners, commonly encountered in cell biology, represent challenging systems. Indeed, competition among partners cannot be predicted by the analysis of single complexes but should be evaluated in a more realistic scenario. For this undertaking, the integration of multiple and varied data sets is required.

The attempt to measure the outcome of distinct pathways requires direct and quantitative experimental access to the products of signaling reactions, and/or of predictive tools based on experimental observation and theoretical modeling. This is of capital importance for GTPases and other key signaling hubs having a central control on many essential cellular activities (Bourne et al. 1991; Scheffzek and Ahmadian 2005). Among all GTPase proteins, RAS is recognized having an outstanding role in cellular growth, differentiation and apoptosis because of its control action on multiple signaling pathways (Olson and Marais 2000). RAS ability in orchestrating different cell responses stems

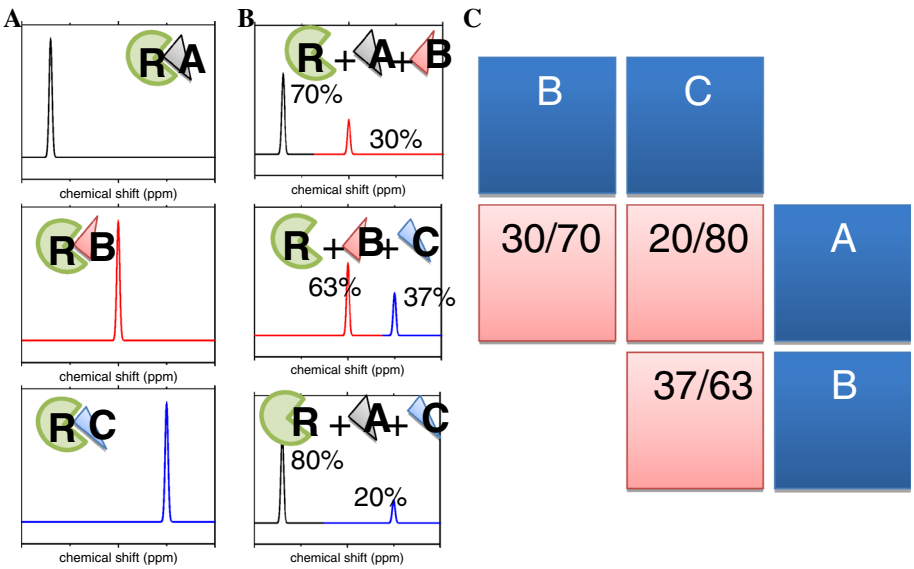

Fig. 1 Example of application of the direct competition experiment to a system comprising a hub protein R and three competitor proteins A, B and C with dissociation constants of 1×10^{-6}; 3×10^{-6}; 6×10^{-6} respectively. The spectra of the individual complexes are recorded (**a**), then the binding proteins are put into direct competition and the ratios between the different bound forms are found (**b**) (Smith and Ikura 2014; Luchinat et al. 2014). This results in three experiments as tabulated in **c**

from its possible interaction with multiple binding partners, in a competitive fashion (Rodriguez-Viciana et al. 2004), and alteration in this complex mechanism is commonly associated to oncogenesis (Bos 1989).

The predictive success of a model of a signaling pathway is largely based on the knowledge of the relative affinity between competing effectors and inhibitors that eventually lead to the definition of an interaction hierarchy. Recently, Smith and Ikura (2014) have proposed an experimental approach for sorting RAS effectors on the basis of their relative affinity. Direct pairwise competition experiments between the selected RAS effectors were used to devise an interaction hierarchy. Through this method, a pathologically relevant mutation of RAS was shown to display altered affinities with the competing effectors, with a subsequent reordering of the hierarchy. In this communication we derive the equations for the treatment of simultaneous equilibria, and we show that the relative amounts of protein complexes formed at the chemical equilibria, which are available through direct pairwise competition NMR experiments, can be used to experimentally derive the relative affinity constants. In turn, the latter can be used for predicting binding scenarios from given starting conditions.

Treatment of simultaneous equilibria

The direct competition method proposed by Smith and Ikura (2014) follows a very simple scheme, reported in Fig. 1. N partner proteins (competitors) are selected, and each one is equilibrated separately with the target hub protein. NMR spectra of the hub protein are recorded and some unique features of the spectrum of each complex are identified and further used as a "fingerprint" of the complex (Fig. 1a). For instance, in the ^{1}H–^{15}N HSQC spectra, distinctive peaks of the hub protein which are chemically shifted in different positions upon binding to the different partner proteins can be selected. The N competitors are then equilibrated pairwise with the hub protein, the NMR spectra are acquired and the relative amount of the two complexes is obtained by the relative intensity of the fingerprint peaks (Fig. 1b), in the assumption that the hub protein is quantitatively bound. This results in recording $N(N-1)/2$ NMR experiments (Fig. 1c). $N-1$ experiments would in principle be enough to fully determine the system, although redundancy makes the method robust to experimental uncertainty.

In the original description (Smith and Ikura 2014), the ratios between the bound forms of the hub protein to each of the two competitors were averaged to give a direct measure of the average affinity of each partner in any mix. The rank of average affinity of each partner was used to define the interaction hierarchy between the partners themselves.

The treatment of the simultaneous equilibria that govern this system can on the other hand provide a direct estimation of the relative dissociation constants between all protein–protein complexes and thus a quantitative description of the species which are formed at some given concentrations (Baeza-Baeza and García-Álvarez-Coque 2011, 2012; Bindel 2007; Vander Griend 2011).

In order to determine the ratios of the dissociation constants from the experimental concentrations of the protein complexes, the intensity ratios between pairs of complexes can be related to their dissociation constants through the relationship:

$$\frac{[RB]}{[RA]} = \frac{[R][B]}{K_B}\frac{K_A}{[R][A]} = \frac{[B]K_A}{[A]K_B} \tag{1}$$

After some algebraic manipulation, as reported in the Supplementary Material, Eq. 2 is obtained:

$$\left(\frac{K_B}{K_A} - 1\right)[RB]^2 + [RB]\left[C + C_R + \frac{K_B}{K_A}(C - C_R)\right] - CC_R = 0 \tag{2}$$

where $C = C_A = C_B$ is the analytical concentration of the competing binding proteins and C_R is the analytical concentration of the hub protein. [RB] is experimentally determined as the ratio between the intensity of the peak corresponding to the RB complex and the sum of the intensities of the peaks corresponding to all species, and multiplied by C_R. It is convenient to define the normalized quantities $f_{BA} = \left(\frac{[RB]}{C_R}\right)_A$, which represents the actual observables, i.e., the percentage of the hub protein R bound to the protein B when in competition with the protein A.

In principle it is possible to determine the ratio $\frac{K_B}{K_A}$ by solving Eq. 2 to obtain

$$\frac{K_B}{K_A} = \frac{\left(\frac{C-[RB]}{C_R}\right)\left(1 - \frac{[RB]}{C_R}\right)}{\frac{[RB]}{C_R}\left(\frac{C+[RB]}{C_R} - 1\right)} = \frac{\left(\frac{C}{C_R} - f_{BA}\right)(1 - f_{BA})}{f_{BA}\left(\frac{C}{C_R} + f_{BA} - 1\right)} \tag{3}$$

However, in order to increase the accuracy of the calculated ratios of the dissociation constants, it is advisable to perform experiments and then analyze simultaneously the results of all pairwise combinations of the binding proteins to take advantage of the relations that link all the $\frac{K_Y}{K_X}$ ratios. The following system of N(N − 1)/2 equations is thus obtained:

$$\left(\frac{K_Y}{K_X} - 1\right)f_{YX}^2 + f_{YX}\left[\frac{C}{C_R} + 1 + \frac{K_Y}{K_X}\left(\frac{C}{C_R} - 1\right)\right] - \frac{C}{C_R} = 0; \quad \text{for } X = 1,\ldots,N; \quad Y = 1,\ldots,N; \quad X \neq Y \tag{4}$$

that can be solved for the N − 1 values of the dissociation constant ratios $\frac{K_Y}{K_X}$. Here $f_{YX} = \left(\frac{[RY]}{C_R}\right)_X$ is the percentage of R bound to Y in the competition with X. Given the presence of experimental uncertainty, this can simply be accomplished by minimizing (for instance by Powell or the Newton algorithm) the discrepancy between all the calculated and experimental ratios.

Once the ratios between the dissociation constants are available, it is possible to predict the distribution of the concentrations within any mix of the considered proteins. Noting that the dissociation constants are interrelated by the competition for R, since

$$[R] = C_R - \sum_{X=1}^{N}[RX] \tag{5}$$

the dissociation constant for the y-th protein can be written as:

$$K_Y = \frac{\left(C_R - \sum_{X=1}^{N}[RX]\right)[Y]}{[RY]} \tag{6}$$

Equation 6 can be rearranged (as described in the Supplementary Material) to get a system of N − 1 equations (for Y = 1, …, N; Y ≠ Z) as the following:

$$f_Y = \frac{f_Z\frac{C_Y}{C_R}}{\frac{C_Z}{C_R}\frac{K_Y}{K_Z} + f_Z\left(1 - \frac{K_Y}{K_Z}\right)} \tag{7}$$

where f_Y and f_Z are the percentage of R bound to Y and Z, respectively, in the presence of any mixture of the binding proteins. Equation 7 can be solved to find the N unknowns (f_X, for X = 1, …, N) by imposing the further constraint that $C_R = \sum_{X=1}^{N}[RX]$, i.e., $\sum_{X=1}^{N} f_X = 1$. The system can be extended to N(N − 1)/2 equations by considering that Z ranges from 1 to N. It is to be noted that the result is independent of the absolute values of the dissociation constants, but rather depends only on their ratios, as long as a quantitative binding of the hub protein is established.

Numerical approach to this problem is simplified by solving the following system of second degree equations which can be easily accomplished by the Newton method as described in the Supplementary Material:

$$f_Y^2 + \left(\sum_{X\neq Y} f_X - \frac{C_Y + K_Y}{C_R} - 1\right)f_Y + \frac{C_Y}{C_R} - \frac{\sum_{X\neq Y} f_X C_Y}{C_R} = 0 \tag{8}$$

Using this approach, it is necessary to fix the smallest K_Y to an arbitrary value (hereon K_0), sufficient to ensure quantitative binding, although the results are independent on this value if such constraint is satisfied, as made evident by Eq. 7. It is important to notice that the treatment described in Eq. 8 can be applied also in the case of non quantitative binding, although in this case the value of K_0 must be known.

As already indicated, rigorous resolution of this and similar systems, representing coupled equilibria, can be accomplished via the Newton method. The relevant expression for the Jacobian matrix is given in the Supplementary Material. Solution may also be sought through approximations. In particular, Eq. 8 simplifies to a first degree equation if $[RY]$ is negligible with respect to C_Y. This approach can also be used in a recursive fashion, approximately as long as $[RY] < 0.2C_Y$ (otherwise, the method tends to diverge, with markedly gross errors).

Table 1 Ratios of the dissociation constants in the performed 3-component synthetic test

	Synthetic value	Calculated value at 0.01 error	Calculated value at 0.02 error	Calculated value at 0.05 error	Calculated value at 0.10 error
$\frac{K_B}{K_A}$	3	3.0 ± 0.1	3.0 ± 0.2	3.1 ± 0.4	3.2 ± 1.0
$\frac{K_C}{K_A}$	6	6.1 ± 0.2	6.1 ± 0.4	6.2 ± 1.0	6.5 ± 2.2

Results and discussion

Synthetic example: three competing partners

A synthetic test was built, in which three partners are interacting with the same protein. The dissociation constants were set to $1 \times 10^{-6}, 3 \times 10^{-6}$ and 6×10^{-6} for the competitors A, B and C, respectively. A system with these constants, assuming a concentration of 0.1 M for the hub protein and 0.2 M for the competitors in the pairwise NMR experiments, would give rise to ratios in the NMR peaks as reported in Fig. 1c.

With these ratios, the system of Eq. 4 becomes:

$$\begin{aligned}
&\left(\frac{K_B}{K_A}-1\right)(0.3)^2+(0.3)\left[3+\frac{K_B}{K_A}(2-1)\right]-2=0;\\
&\left(\frac{K_C}{K_A}-1\right)(0.2)^2+(0.2)\left[3+\frac{K_C}{K_A}(2-1)\right]-2=0;\\
&\left(\frac{K_C}{K_B}-1\right)(0.37)^2+(0.37)\left[3+\frac{K_C}{K_B}(2-1)\right]-2=0;
\end{aligned} \tag{9}$$

and the ratios between the constants are thus found to be $\frac{K_B}{K_A}=3$; $\frac{K_C}{K_A}=6$; $\frac{K_C}{K_B}=2$.

In order to check the stability of the solution, we have repeated the calculation 1,000 times by introducing a random error of 0.01, 0.02, 0.05 or 0.10 in the f_{YX} values. The results are reported in Table 1. The standard deviations of the values obtained over the 1,000 iterations are given as errors. These calculations show that the results are accurate even for experimental errors of 5–10 %, which may actually affect the data, although the standard deviation is relatively large in these cases.

Once the ratios between the constants are available, it is possible to devise the relative amounts of the complex in any arbitrary mix of the components. In the present case we have chosen to calculate the distribution of the species as a function of the analytical concentration of components A and B when component C is set to a concentration $C_C = 4C_R$.

Subsequently, the concentration of the 3 bound species are found by solving with the Newton approach the system of Eq. 8, that is now in the form:

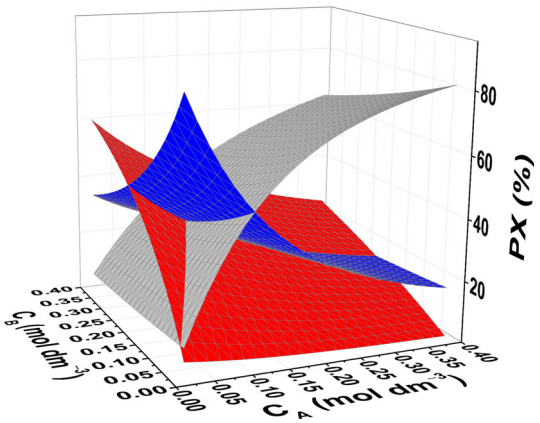

Fig. 2 Percentage of RA, RB and RC for changing analytical concentration of A and B, in the presence of 0.1 M R and 0.4 M C, as derived from (Luchinat et al. 2014). *Grey*: [RA], *red*: [RB], *blue*: [RC]

$$\begin{aligned}
&[RA]^2+\left(\sum_{I\neq J}[RI]-C_A-0.1-K_A\right)[RA]+0.1C_A\\
&\quad-\sum_{I\neq J}[RI]C_A=0;\\
&[RB]^2+\left(\sum_{I\neq J}[RI]-C_B-0.1-K_B\right)[RB]+0.1C_B\\
&\quad-\sum_{I\neq J}[RI]C_A=0;\\
&[RC]^2+\left(\sum_{I\neq J}[RI]-0.3-K_C\right)[RC]+0.04\\
&\quad-\sum_{I\neq J}[RI]C_A=0;
\end{aligned}$$

Figure 2 reports the outcome of the calculation, performed by fixing the highest dissociation constant (i.e., that of the complex with lower affinity) to $K_C = 6 \times 10^{-8}$. The discrepancies between the values calculated with either $K_C = 6 \times 10^{-8}$ or with the "correct" value of $K_C = 6 \times 10^{-6}$ are below 0.001 %, and are likely due to computational round off errors.

Experimental example: 9 RAS-binding domains competing for RAS

The same kind of calculations can be performed for the case of the experimental data reported in (Smith and Ikura

Table 2 Ratios between the dissociation constants of the different competitors in the presence of the wild type or G12V RAS

	WT RAS	G12V RAS
$\frac{K_{RIN1}}{K_{BRAF}}$	10.9 ± 6.2	6.2 ± 1.8
$\frac{K_{ARAF}}{K_{BRAF}}$	13.5 ± 7.7	15.6 ± 4.8
$\frac{K_{Plce1-2}}{K_{BRAF}}$	15.5 ± 8.9	7.9 ± 2.3
$\frac{K_{RGL1}}{K_{BRAF}}$	18 ± 10	3.1 ± 0.9
$\frac{K_{RASSF5}}{K_{BRAF}}$	27 ± 16	9.2 ± 2.7
$\frac{K_{RALGDS}}{K_{BRAF}}$	66 ± 40	13.4 ± 4.0
$\frac{K_{AF6-1}}{K_{BRAF}}$	380 ± 270	35 ± 11
$\frac{K_{RGS14-1}}{K_{BRAF}}$	~10,000	400 ± 270

2014). In this paper, two sets of experiments were described, in which nine partners were competing for the RAS hub protein. In the first set of experiments the protein was in the wild type form, in the second set the G12V variant of RAS was used. A total of 29 and 31 ratios from direct competition NMR experiments were measured in the two cases, respectively, with a concentration of 0.1 M for the hub protein and 0.2 M for the competitors.

Following the same steps as described above in the case of three partners, the ratios between the dissociation constants were calculated using Eq. 4 (see Table 2). The agreement between experimental and back-calculated ratios in the concentration of formed complexes for all pairwise experiments is shown in Figures 3 and S1-S2. The agreement is good and the consistency among the whole series of experiments proves the robustness of the method. The average discrepancy between best-fit and experimental data is 8 and 6 % for the wild type and the mutant RAS, respectively (with 5/29 signals of the wild type and 3/31 signals of the mutant showing an error larger than 15 %). Experimental and back-calculated relative amounts of the complex of RAS with the different competitors in all pairwise experiments are also reported in Tables 3 and 4. The much lower binding constant of RGS14-1 with respect to the other partners makes it difficult to detect the complex between RAS and this protein in the presence of stronger competitors and in this case it was possible to determine only the order of magnitude of the dissociation rate ratios.

After determining the ratios between the constants, it is possible to calculate the concentration of all the various species under different starting conditions. Figures 4 and S3-S4 show the fraction of RAS bound to different competitors when applied in a 1:4 ratio with a mixture of competitors. The concentration of one selected competitor is changed within the mix while, for simplicity, all other components have equal concentration among them, with the constraint that the sum of the analytical concentrations

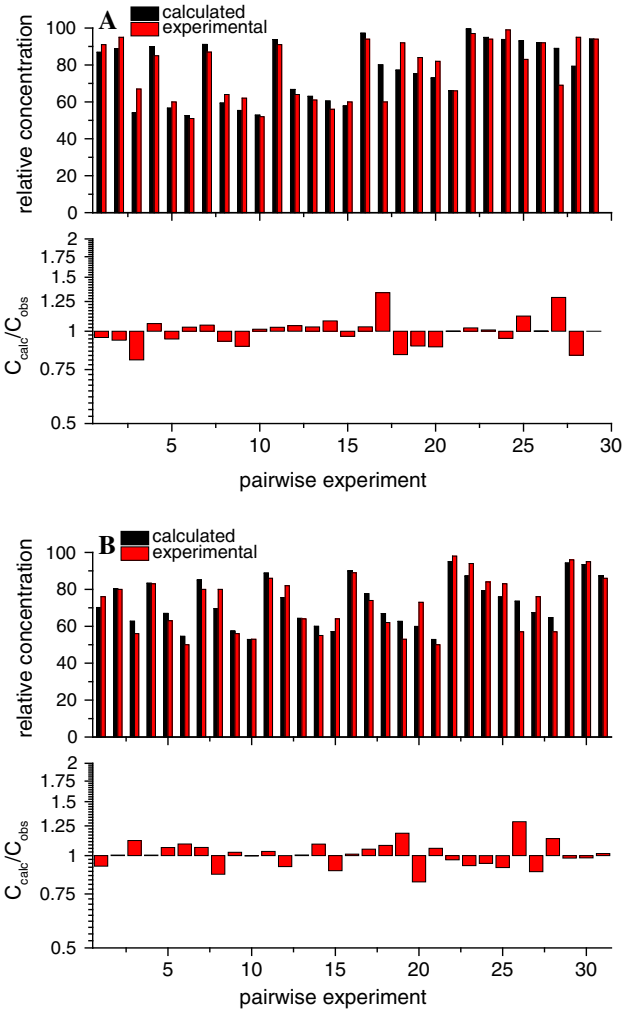

Fig. 3 Agreement between experimental and back-calculated ratios in the concentration of formed complexes for all pairwise experiments with the wild type RAS (**a**) and the G12V mutant (**b**). The experimental ratio in the concentration of each complex is determined from the relative amount of the two complexes formed when two competitors are equilibrated with the hub protein. This relative amount was obtained from the relative intensity of the fingerprint peaks, in the assumption that the hub protein is quantitatively bound (Smith and Ikura 2014). Experiments are numbered as in Tables 2, 3

of all competitors is 4 times larger than the concentration of RAS. Panels A-I in Figures S3-S4 show all concentration profiles calculated for the nine competitors by changing their molar fraction in the competitors mixture with either the wild type or the mutant RAS, and Fig. 4a–c shows some representative examples for the mutant RAS. Figures 4d, S3J and S4J summarize the concentration profiles of each competitor analogously to what calculated in Fig. 2e in (Smith and Ikura 2014): this is helpful to quickly recover the interaction hierarchy, comparing the values of each curve at any given point (50 % in analogy to what is done in Smith and Ikura 2014). Notably, the same interaction hierarchies determined in (Smith and Ikura

Table 3 Pairwise competition data for effector domains and RAS (Smith and Ikura 2014)

	BRAF	RIN1	ARAF	Plcε1-2	RGL1	RASSF5	RALGDS	AF6-1
RIN1	1: 91 % (87 %)							
ARAF	2: 95 % (89 %)	3: 67 % (54 %)						
Plcε1-2	4: 85 % (90 %)	5: 60 % (57 %)	6: 51 % (53 %)					
RGL1	7: 87 % (91 %)	8: 64 % (59 %)	9: 62 % (55 %)	10: 52 % (53 %)				
RASSF5	11: 91 % (94 %)	12: 64 % (67 %)	13: 61 % (63 %)	14: 56 % (61 %)	15: 60 % (58 %)			
RALGDS	16: 94 % (97 %)	17: 60 % (80 %)	18: 92 % (77 %)	19: 84 % (75 %)	20: 82 % (73 %)	21: 66 % (66 %)		
AF6-1	22: 97 % (99 %)	23: 94 % (95 %)	24: 99 % (94 %)	25: 83 % (93 %)	26: 92 % (92 %)	27: 69 % (89 %)	28: 95 % (79 %)	
RGS14-1								29: 94 % (94 %)

The table provides the experiment number and the experimental and back-calculated (in parenthesis) relative amount of the complex of RAS with the effector indicated on the top of the column, in the presence of the effector indicated on the left of the row

Table 4 Pairwise competition data for effector domains and G12V RAS (Smith and Ikura 2014)

	BRAF	RGL1	RIN1	Plcε1-2	RASSF5	RALGDS	ARAF	AF6-1
RGL1	1: 76 % (70 %)							
RIN1	2: 80 % (80 %)	3: 56 % (63 %)						
Plcε1-2	4: 83 % (83 %)	5: 63 % (67 %)	6: 50 % (55 %)					
RASSF5	7: 80 % (85 %)	8: 80 % (70 %)	9: 56 % (57 %)	10: 53 % (53 %)				
RALGDS	11: 86 % (89 %)	12: 82 % (76 %)	13: 64 % (64 %)	14: 55 % (60 %)	15: 64 % (57 %)			
ARAF	16: 89 % (90 %)	17: 74 % (78 %)	18: 62 % (67 %)	19: 53 % (63 %)	20: 73 % (60 %)	21: 50 % (53 %)		
AF6-1	22: 98 % (95 %)	23: 94 % (87 %)	24: 84 % (79 %)	25: 83 % (76 %)	26: 57 % (74 %)	27: 76 % (67 %)	28: 57 % (65 %)	
RGS14-1						29: 96 % (94 %)	30: 95 % (94 %)	31: 86 % (87 %)

The table provides the experiment number and the experimental and back-calculated (in parenthesis) relative amount of the complex of RAS with the effector indicated on the top of the column, in the presence of the effector indicated on the left of the row

2014) for wild type and G12V RAS were obtained, as expected from the fact that the same NMR data have been analyzed.

The calculated ratios between dissociation constants (and thus the interaction hierarchy) deviate to some extent from the values determined through ITC experiments (Smith and Ikura 2014). Such differences may be due to the different experimental conditions between ITC and NMR measurements. On the other hand, it is worthy to note that the small discrepancies between the observed and calculated relative concentrations shown in Fig. 3 (6–8 %) can be due to the experimental uncertainty in the NMR measurements, which may be of this order. These discrepancies actually reflect in the errors in the ratios of the dissociation constants reported in Table 2 (and in line with the synthetic data calculations in Table 1). Further warning is represented by the possible presence of kinetic effects, which may affect the concentration of the different complexes, and of interactions between the binding proteins themselves, which may have the effect of decreasing the effective protein concentration.

Despite the limitation in the use of this approach, the method is of extreme interest for its immediate application in the investigation of all cases in which similar interaction partners compete for the same binding site with similar affinities, as in the case of drug screening (Bertini et al. 2005; Borsi et al. 2010; Harner et al. 2013; Nazaré et al. 2012; Pellecchia et al. 2008).

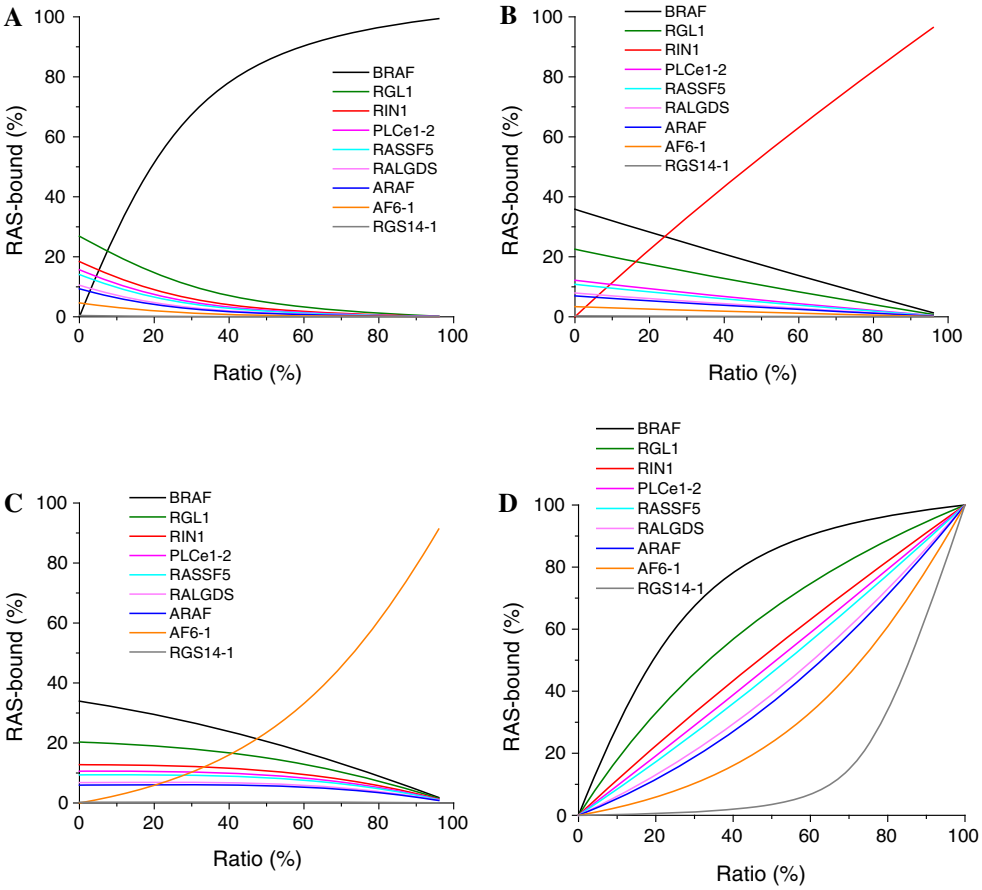

Fig. 4 Concentration profiles calculated for a mixture of competitors in 4:1 excess with respect to G12V RAS. The concentration of one competitor at a time is varied in the mixture (**a**–**c**) and the percentage of RAS bound to the selected competitor is calculated. **d** Summarizes the concentration of all the competitors. The order of the curves at any percentage is related to the affinity of the competitors for RAS, thus gives access to the interaction hierarchy

Conclusions

The approach of Smith and Ikura (2014) of direct competition experiments to devise the relative affinities of any given number of partners to a hub protein provides a powerful tool for quantitative systems biology and an attractive target for a quantitative description in terms of simultaneous equilibria. By both synthetic and experimental examples, we have shown that such pairwise competition experiments provide all the information needed not only to sort the interaction partners but also to quantitatively predict the relative amount of the possible complexes in any given mixture of competing proteins.

Acknowledgments Discussions with M. Ikura and M. Smith are acknowledged. C. Luchinat is acknowledged for support and encouragement. This work has been supported by Ente Cassa di Risparmio di Firenze, EC Bio-NMR No. 261863, BioMedBridges No. 284209, and EU ESFRI Instruct Core Centre CERM, Italy.

References

Baeza-Baeza JJ, García-Álvarez-Coque MC (2011) Systematic approach to calculate the concentration of chemical species in multi-equilibrium problems. J Chem Educ 88:169–173

Baeza-Baeza JJ, García-Álvarez-Coque MC (2012) Systematic approach for calculating the concentrations of chemical species in multiequilibrium problems: inclusion of the ionic strength effects. J Chem Educ 89:900–904

Bertini I, Fragai M, Giachetti A, Luchinat C, Maletta M, Parigi G, Yeo KJ (2005) Combining in silico tools and NMR data to validate protein-ligand structural models: application to matrix metalloproteinases. J Med Chem 48:7544–7559

Bindel TH (2007) Discovering the thermodynamics of simultaneous equilibria. An entropy analysis activity involving consecutive equilibria. J Chem Educ 84:449

Borsi V, Calderone V, Fragai M, Luchinat C, Sarti N (2010) Entropic contribution to the linking coefficient in fragment based drug design: a case study. J Med Chem 53:4285–4289

Bos JL (1989) RAS oncogenes in human cancer: a review. Cancer Res 49:4682–4689

Bourne HR, Sanders DA, McCormick F (1991) The GTPase superfamily: conserved structure and molecular mechanism. Nature 349:117–127

Harner MJ, Frank AO, Fesik SW (2013) Fragment-based drug discovery using NMR spectroscopy. J Biomol NMR 56:65–75

Kholodenko BN, Hancock JF, Kolch W (2010) Signalling ballet in space and time. Nat Rev Mol Cell Biol 11:414–426

Kitano H (2002) Systems biology: a brief overview. Science 295:1662–1664

Luchinat C, Parigi G, Ravera E (2014) NMR technology: the competitive world of RAS biology. Nat Chem Biol 10:173–174

Nazaré M, Matter H, Will DW, Wagner M, Urmann M, Czech J, Schreuder H, Bauer A, Ritter K, Wehner V (2012) Fragment deconstruction of small, potent factor Xa inhibitors: exploring

the superadditivity energetics of fragment linking in protein-ligand complexes. Angew Chem Int Ed Engl 51:905–911

Olson MF, Marais R (2000) Ras protein signalling. Semin Immunol 12:63–73

Papin JA, Hunter T, Palsson BO, Subramaniam S (2005) Reconstruction of cellular signalling networks and analysis of their properties. Nat Rev Mol Cell Biol 6:99–111

Pellecchia M, Bertini I, Cowburn D, Dalvit C, Giralt E, Jahnke W, James TL, Homans SW, Kessler H, Luchinat C et al (2008) Perspectives on NMR in drug discovery: a technique comes of age. Nat Rev Drug Discov 7:738–745

Rodriguez-Viciana P, Sabatier C, McCormick F (2004) Signaling specificity by Ras family GTPases is determined by the full spectrum of effectors they regulate. Mol Cell Biol 24:4943–4954

Scheffzek K, Ahmadian MR (2005) GTPase activating proteins: structural and functional insights 18 years after discovery. Cell Mol Life Sci CMLS 62:3014–3038

Smith MJ, Ikura M (2014) Integrated RAS signaling defined by parallel NMR detection of effectors and regulators. Nat Chem Biol 10:223–230

Vander Griend DA (2011) Equilibrator: modeling chemical equilibria with excel. J Chem Educ 88:1727–1729